Published in final edited form as:
Cancer Res. 2014 November 1; 74(21): 6184–6193. doi:10.1158/0008-5472.CAN-14-1357.

Genetic deletion of AEG-1 prevents hepatocarcinogenesis

Chadia L. Robertson[1,2], **Jyoti Srivastava**[1], **Ayesha Siddiq**[1], **Rachel Gredler**[1], **Luni Emdad**[1], **Devaraja Rajasekaran**[1], **Maaged Akiel**[1], **Xue-Ning Shen**[1], **Chunqing Guo**[1], **Shah Giashuddin**[3], **Xiang-Yang Wang**[1], **Shobha Ghosh**[4], **Mark A Subler**[1], **Jolene J. Windle**[1,5], **Paul B. Fisher**[1,5,6], and **Devanand Sarkar**[1,5,6,7]

[1]Department of Human and Molecular Genetics, Virginia Commonwealth University, Richmond, VA

[2]Department of Biochemistry, Virginia Commonwealth University, Richmond, VA

[3]Department of Pathology, New York Hospital Medical Center, Flushing, NY

[4]Department of Internal Medicine, Virginia Commonwealth University, Richmond, VA

[5]Massey Cancer Center, Virginia Commonwealth University, Richmond, VA

[6]VCU Institute of Molecular Medicine, Virginia Commonwealth University, Richmond, VA

Abstract

Activation of the oncogene AEG-1 (MTDH, LYRIC) has been implicated recently in the development of hepatocellular carcinoma (HCC). In mice, HCC can be initiated by exposure to the carcinogen DEN, which has been shown to rely upon activation of NF-κB in liver macrophages. Since AEG-1 is an essential component of NF-κB activation, we interrogated the susceptibility of mice lacking the AEG-1 gene to DEN-induced hepatocarcinogenesis. AEG-1-deficient mice displayed resistance to DEN-induced HCC and lung metastasis. No difference was observed in the response to growth factor signaling or activation of Akt, ERK and β-catenin, compared to wild-type control animals. However, AEG-1-deficient hepatocytes and macrophages exhibited a relative defect in NF-κB activation. Mechanistic investigations showed that IL-6 production and STAT-3 activation, two key mediators of HCC development, were also deficient along with other biological and epigenetics findings in the tumor microenvironment confirming that AEG-1 supports an NF-κB-mediated inflammatory state that drives HCC development. Overall, our findings offer *in vivo* proofs that AEG-1 is essential for NF-κB activation and hepatocarcinogenesis, and they reveal new roles for AEG-1 in shaping the tumor microenvironment for HCC development.

Keywords

Astrocyte elevated gene-1 (AEG-1); hepatocellular carcinoma (HCC); tumor microenvironment; macrophages; NF-κB

[7]Corresponding author: 1220 E Broad St., PO Box 980035, Richmond, VA 23298; Tel: 804-827-2339; Fax: 804-628-1176; dsarkar@vcu.edu.

Disclosure: All authors have no potential conflicts.

Introduction

Hepatocellular carcinoma (HCC) is a highly fatal disease with mortality running parallel to its incidence (1). In the majority of cases HCC arises in a setting of chronic inflammation, such as infection with HBV or HCV, alcoholism and non-alcoholic fatty liver disease (NAFLD) (1, 2). NF-κB is a key transcriptional regulator of the inflammatory response and plays an essential role in regulating inflammatory signaling in the liver (3, 4). NF-κB activation is a frequent and early event in human HCC of viral and non-viral etiologies and has been attributed to the acquisition of transformed phenotype during hepatocarcinogenesis (5–9). Both HBV X protein (HBX) and HCV core protein have been shown to activate NF-κB by multiple mechanisms (7, 10, 11). Many patients with advanced liver disease present with increased levels of LPS, resulting in activation of NF-κB in the liver (12). Fatty acids may also activate NF-κB in NAFLD patients (13).

The role of NF-κB in HCC development and progression has been interrogated in several mouse models. Mdr2−/− mice develop spontaneous cholestatic hepatitis and HCC (3). Overexpression of a non-degradable mutant IκBα that blocks NF-κB activation significantly inhibited HCC progression in this model (3). Hepatocyte-specific knockout of IKKβ abrogated HCC development in a transgenic mouse overexpressing lymphotoxin α and/or β(14). These findings indicate that NF-κB activation in hepatocytes is necessary in inflammation-induced HCC. In contrast, hepatocyte-specific knockout of IKKβ promoted HCC development in N-nitrosodiethylamine (DEN)-initiation model and hepatocyte-specific knockout of IKKγ (NEMO) resulted in spontaneous development of HCC (15, 16). ROS-induced JNK and STAT3 activation has been suggested to promote HCC in IKKβ knockout model and IKKβ has been suggested to inhibit both hepatic injury and proliferation (17). However, deletion of IKKβ in macrophages significantly abrogated DEN-induced HCC (15). Additionally genetic deletion of IL-6 or inhibition of inflammatory cytokines, such as TNF-α, provided a significant reduction in tumor load (18). Injury to hepatocytes, such as those caused by DEN, leads to release of IL-1α that activates NF-κB in liver macrophages (Kupffer cells) with subsequent release of cytokines, such as IL-6 (18–20). IL-6 promotes proliferation and survival of hepatocytes by activating STAT-3 signaling(18). Thus, NF-κB activation in the tumor microenvironment plays a fundamental role in hepatocarcinogenesis.

Astrocyte Elevated Gene-1 (AEG-1), also known as Metadherin (MTDH) and LYRIC, is an oncogene that is overexpressed in all cancers (21). AEG-1 overexpression is detected with the progression of cancer, especially in the aggressive metastatic stage, and negatively correlates with poor survival and overall adverse prognosis (21). *In vitro* studies and investigations using nude mice xenograft and metastatic models with diverse cancer cell lines documented that AEG-1 overexpression induces an aggressive, angiogenic and metastatic phenotype whereas knockdown of AEG-1 inhibits proliferation and invasion and markedly abrogates tumor growth and metastasis (22–25). AEG-1 plays an important role in regulating hepatocarcinogenesis. We documented that AEG-1 is overexpressed at both mRNA and protein levels in a high percentage (>90%) of HCC patients and a significant percentage of patients harbored genomic amplification of the AEG-1 locus in chromosome 8q22 (22). AEG-1 is transcriptionally regulated by c-Myc (26), an oncogene frequently upregulated in HCC (27). The tumor suppressor miRNA miR-375, which is downregulated

in HCC patients, targets AEG-1 (28). Thus AEG-1 overexpression occurs by multiple mechanisms in HCC patients. HCC with more microvascular invasion or pathologic satellites, poorer differentiation, and TNM stages II to III are prone to exhibit higher AEG-1 expression (29). HCC patients with high AEG-1 expression documented higher recurrence and poor overall survival (29, 30). Overexpression of AEG-1 in a poorly aggressive HCC cell line HepG3, which expresses low level of AEG-1, significantly increases *in vitro* proliferation, invasion and anchorage-independent growth and *in vivo* tumorigenesis, angiogenesis and metastasis in nude mice (22). Conversely, knockdown of AEG-1 in highly aggressive QGY-7703 cells, expressing high levels of AEG-1, significantly abrogates *in vivo* tumorigenesis (22, 31). We have shown that transgenic mice with hepatocyte-specific overexpression of AEG-1 (Alb/AEG-1) do not show spontaneous HCC but develop highly aggressive angiogenic HCC with significantly accelerated kinetics upon treatment with DEN when compared to their WT counterparts (32). AEG-1 overexpression profoundly modulates expression of genes associated with proliferation, invasion, chemoresistance, angiogenesis and metastasis in both human HCC cell lines and Alb/AEG-1 hepatocytes (22, 32).

Multiple pro-survival signaling pathways, such as NF-κB, PI3K/Akt, Wnt/β-catenin and MEK/ERK, become activated upon overexpression of AEG-1 in human cancer cells and Alb/AEG-1 hepatocytes (22, 32). Pharmacological and genetic inhibition studies have elucidated the importance of all these signaling pathways in mediating AEG-1-induced oncogenesis (22). However, apart from NF-κB, the molecular mechanism by which AEG-1 activates these signaling pathways is not known. More importantly, whether AEG-1 is required for activation of these pathways under physiological conditions has not been investigated. We have documented that AEG-1 directly interacts with the p65 subunit of NF-κB and CBP thereby functioning as a bridging factor between NF-κB and basal transcriptional machinery promoting NF-κB-induced transcription (33, 34). A recent study has documented that AEG-1, anchored on the ER membrane, associates with upstream ubiquitinated activators of NF-κB, such as RIP1 and TRAF2, facilitating their accumulation and subsequent NF-κB activation (35).

In the present study, we analyzed the response of AEG-1 knock-out (AEG-1KO) mouse to DEN-induced HCC development and progression. Our experiments unravel a fundamental role of AEG-1 in regulating NF-κB activation, especially in the tumor microenvironment, thereby rendering AEG-1KO mice to be significantly resistant to initiation and progression of HCC.

Materials and methods

Mouse model

AEG-1KO mouse was generated in C57BL/6:129/Sv background and the procedure is described in detail in the supplement. We have backcrossed the line to C57BL/6 for 10 generations and obtained similar results for both the WT and AEG-1KO mice on the C57BL/6 background as on the C57BL/6:129/Sv background. AEG-1KO mice were viable and fertile, although litter sizes were very small (1–2 pups per litter). Further, even litters generated by crossing AEG-1+/− breeding pairs were very small (2–3 pups per litter), which precluded generating large numbers of WT and AEG-1KO mice as littermates. Therefore,

the majority of the experiments were carried out with age-matched mice generated by breeding WT and AEG-1KO mice separately. However, it should be noted that the same phenotypes were observed in AEG-1KO mice generated from AEG-1+/− X AEG-1+/− matings as from AEG-1KO X AEG-1KO matings. Thus our findings are not restricted to strains or littermates. All animal studies were approved by the Institutional Animal Care and Use Committee at Virginia Commonwealth University, and were conducted in accordance with the Animal Welfare Act, the PHS Policy on Humane Care and Use of Laboratory Animals, and the U.S. Government Principles for the Utilization and Care of Vertebrate Animals Used in Testing, Research, and Training.

Cell culture

Primary mouse hepatocytes were isolated as described (32) and were cultured in Williams E medium containing $NaHCO_3$, L-glutamine, insulin (1.5 μM) and dexamethasone (0.1 μM) at 37°C and in 5% CO_2. For isolating primary perinoeal macrophages, mice were injected i.p. with 4% thioglycollate and 4 days later macrophages were harvested in PBS via i.p. injection. Macrophages were cultured in Dulbecco's Modified Eagle's Medium with 10% fetal calf serum at 37°C and in 5% CO_2.

Transient transfection and luciferase assay

For transfections, 1×10^5 hepatocytes were plated in 24-well collagen coated plates and the next day transfected using Promofectin-Hepatocyte transfection reagent in 9:1 ratio of NF-κB luciferase reporter plasmid and renilla luciferase reporter plasmid. After 48 hours, cells were treated with LPS (200 ng/ml) for 24 h. Luciferase assays were measured using Dual Luciferase Reporter Assay kit (Promega) following manufacturer's protocol and firefly luciferase activity was normalized by renilla luciferase activity. Each experiment was performed in triplicates and three times to calculate means and standard errors.

Total RNA extraction, cDNA preparation and Real time PCR

Total RNA was extracted from hepatocytes, macrophages or mouse tissues using the QIAGEN miRNAeasy Mini Kit (QIAGEN, Valencia, CA). cDNA preparation was done using ABI cDNA synthesis kit (Applied Biosystems, Foster City, CA). Real-time polymerase chain reaction (RT-PCR) was performed using an ABI ViiA7 fast real-time PCR system and Taqman gene expression assays according to the manufacturer's protocol (Applied Biosystems, Foster City, CA).

RNA sequencing (RNA-Seq)

Total RNA, extracted using Qiagen miRNAeasy mini kit (Qiagen, Valencia, CA) from livers of 3 adult mice per group, was employed for RNA sequencing. RNA-Seq library was prepared using Illumina TruSeq RNA sample preparation kit and sequenced on Illumina HiSeq2000 platform. RNA-Seq libraries were pooled together to aim about 25–40M read passed filtered reads per sample. All sequencing reads were aligned with their reference genome (UCSC mouse genome build mm9) using TopHat2 and the Bam files from alignment were processed using HTSeq-count to obtain the counts per gene in all samples. The counts were read into R software using DESeq package and plot distributions were

analyzed using Reads Per Kilobase Million (RPKM) values. Data were filtered based on low count or low RPKM value (<40 percentile). Pairwise tests were performed between each group using the functions in DESeq. Genes showing log2 fold-change of >1.5 or <−1.5, FDR of <0.1 and p-value of <0.01 were selected.

Statistical analysis

Data were represented as the mean ±Standard Error of Mean (S.E.M) and analyzed for statistical significance using one-way analysis of variance (ANOVA) followed by Newman-Keuls test as a post hoc test.

Results

Aged AEG-1KO mice do not develop spontaneous tumors

We generated an AEG-1KO mouse in which the promoter region, exon 1 and part of intron 1 of the AEG-1 gene was deleted using a Cre-loxP system. The authenticity of AEG-1 knockout was confirmed by Southern blotting, genomic PCR, Taqman Q-RT-PCR, Western blot analyses and immunohistochemistry (Fig. S1). AEG-1KO mice were viable and fertile and developed normally. No histological difference was observed in the internal organs of young AEG-1KO (8–12 weeks old) mice when compared to WT littermates or age-matched WT mice (Fig. 1A). Analysis of bone marrow, peripheral blood cells and spleen cell composition at this age also showed no difference (Table S1, Table S2 and Fig. S2). However, when aged (16 months old), spontaneous tumorigenesis was observed in multiple organs of some WT mice, but none of the AEG-1KO mice showed this phenomenon (n = 20) (Fig. 1A and 1B). Lymphoma and adenocarcinoma were observed in the liver, adenocarcinoma and carcinoid tumors were observed in the lungs and myxoma was observed in the heart of the aged WT mice. Interestingly the spontaneous tumors developing in the livers of WT mice stained strongly for AEG-1, especially those cells invading into the surrounding liver parenchyma, further confirming the essential role of AEG-1 in regulating tumor invasion (Fig. 1C). Marked infiltration of macrophages, evidenced by staining for macrophage marker F4/80, was observed in the aged (16 m old) WT liver but not in AEG-KO liver (Fig. 1D), as well as in aged WT spleen but not in AEG-1KO spleen (Fig. S3). No difference in infiltration of neutrophils, as evidenced by Ly6G staining, was observed between aged WT and AEG-1KO mice (data not shown), suggesting that aging-associated chronic inflammatory responses are blunted in AEG-1KO mice.

AEG-1KO mice are resistant to experimental hepatocarcinogenesis

WT and AEG-1KO mice were given a single i.p. injection of DEN (30 μg/gm) and tumorigenesis was monitored at 32 weeks. Compared to WT mice, AEG-1KO mice showed profound resistance to DEN-induced HCC. AEG-1KO mice either developed no tumor or the tumors were very small (<2mm) (Table S3 and Fig. 2A). WT livers presented with AFP-positive HCC with vascular invasion (arrow in Fig. 2B) and high AEG-1 expression, while the liver architecture was preserved in AEG-1KO mice (Fig. 2B). Serum levels of aspartate aminotransferase (AST), alanine aminotransferase (ALT) and alkaline phosphatase (Alk Phos) were significantly higher in WT mice as compared to AEG-1KO mice indicating liver damage (Fig. 2C). One important aspect of AEG-1 is its ability to induce metastasis. We

therefore tested a more aggressive experimental procedure where tumorigenesis was induced by injection of DEN (10 μg/gm) and then it was promoted by providing phenobarbital (PB; 0.05%) daily in drinking water. Tumorigenesis was monitored at 28 weeks. WT mice exhibited an intensified hepatocarcinogenic response evidenced by large necrotic liver tumors with a 52% rate of lung metastasis (Table 1 and Fig. 2D). AEG-1KO mice remained remarkably resistant even to this combinatorial treatment with no distant metastasis. Histological analysis of liver demonstrated HCC in WT mice (Fig. 2E). Although some level of dysplasia was observed in AEG-1KO mice, frank HCC was not detected. The metastatic nodules in the WT lung were positive for AFP indicating their origin in the liver (Fig. 2F). Staining for macrophage marker F4/80 showed significant infiltration of macrophages both in DEN- and DEN/PB-treated WT tumors but not in AEG-1KO livers (Fig. 2G). Quantification of macrophage infiltration is shown in Fig. S4. We stained DEN-treated WT and AEG-1KO liver for α-smooth muscle actin (α-SMA) as an indicator of activation of stellate cells and fibrogenic response. A substantial increase in α-SMA staining was observed in the tumor in WT mice when compared to non-tumor region (Fig. S5). α-SMA staining in AEG-1KO liver was similar to that in the non-tumor region of WT liver.

A possible cause of the pronounced resistance of AEG-1KO mice to DEN-induced HCC might be improper metabolism of DEN in these mice so that DEN is not capable of adequately damaging hepatocytes. To rule out this possibility we injected WT and AEG-1KO 2 wks old pups with DEN and then measured serum liver enzymes 48 h later. Both WT and AEG-1KO mice showed significant induction of liver enzymes indicating that DEN could damage both hepatocytes in a similar manner (Table S4).

Growth factor signaling is not affected in AEG-1KO mice

Activation of pro-survival signaling pathways, such as PI3K/AKT, MEK/ERK and β-catenin, have been shown to play a role in mediating oncogenic effects of overexpressed AEG-1 in human HCC cells as well as in Alb/AEG-1 mice (22, 32). We treated WT and AEG-1KO hepatocytes with EGF (50 ng/mL) and analyzed temporal activation of EGFR, AKT and ERK1/2. Both WT and AEG-1KO hepatocytes showed similar kinetics and magnitude of activation suggesting that under physiological condition AEG-1 does not modulate growth factor signaling (Fig. 3A). No difference was observed in the activated (phosphorylated) forms of AKT, ERK1/2and β-catenin in adult WT and AEG-1KO liver samples under basal condition (Fig. 3B). These results indicate that AEG-1 is not required for physiological regulation of Akt, ERK1/2 and β-catenin. We next tested activation of these signaling pathways in DEN-treated WT and AEG-1KO liver samples (Fig. 3C). No significant difference was observed in the activation of AKT, ERK1/2 and β-catenin in the two groups. In naïve mice, inhibition in activated STAT3 and p65 NF-κB, known regulators of HCC, was observed in AEG-1KO livers *versus* WT (Fig. 3D). Upon DEN-treatment there was further induction of both p-p65 NF-κB and p-STAT3 in WT mice but not in AEG-1KO mice (Fig. 3D). These findings were confirmed by immunohistochemistry (IHC) in DEN-treated liver samples (Fig. 3E). Upon DEN-treatment a significant increase in IL-6 protein level was observed in liver homogenates of WT mice but not in AEG-1KO mice (Fig. 3F).

NF-κB activation is abrogated in AEG-1KO mice

We measured NF-κB luciferase reporter activity in primary hepatocytes isolated from WT and AEG-1KO mice. Both basal and LPS-induced luciferase activity was significantly blunted in AEG-1KO hepatocytes when compared to WT hepatocytes (Fig. 4A). As a corollary LPS-induced phosphorylation (Fig. 4B) and nuclear translocation (Fig. 4C) of the p65 subunit of NF-κB and induction of NF-κB-target genes IL-1β and IL-6 (Fig. 4D) were significantly abrogated in AEG-1KO hepatocytes versus WT hepatocytes. Since NF-κB activation in macrophages is crucial for HCC, we next analyzed peritoneal macrophages isolated from WT and AEG-1KO mice. AEG-1 mRNA expression in macrophages was significantly higher compared to that in hepatocytes (Fig. 5A). In primary hepatocytes AEG-1 is localized predominantly in the nucleus while in macrophages it is located both in the nucleus and in the cytoplasm (Fig. 5B). Upon LPS treatment nuclear translocation of p65 NF-κB was substantially abrogated in AEG-1KO macrophages compared to WT macrophages (Fig. 5C). LPS-mediated induction of IL-6 and IL-1β was also markedly blunted in AEG-1KO peritoneal macrophages versus WT (Fig. 5D–E). We collected conditioned media (CM) from LPS-treated WT and AEG-1KO hepatocytes and treated WT and AEG-1KO macrophages with the CM. CM from WT hepatocytes induced IL-6 mRNA expression only in WT macrophages but not in AEG-1KO macrophages (Fig. 5F). Additionally CM from AEG-1KO hepatocytes failed to induce IL-6 mRNA in either WT or AEG-1KO macrophages.

To extend these observations further we performed RNA-sequencing analysis using liver samples from WT and AEG-1KO mice. Using cut-off of Log2 fold-change of 1.5 or −1.5, 597 genes showed differential change, out of which 247 genes were upregulated and 350 genes were downregulated in AEG-1KO liver *versus* WT liver (Table S5). These differentially changed genes were analyzed using Ingenuity pathway analysis software. The data were analyzed to identify the upstream regulators the activation or inhibition of which might lead to alterations in downstream genes. An activation z-score >2 indicates activation and a score of <−2 indicates inhibition. The most significant inhibition ($p<0.02$) was observed for genes downstream of IL-6, IL-1B, TNF family, IL17RA and NF-κB complex (Table S6). These upstream regulators were analyzed for regulator effects to predict functional endpoints. It was observed that collective inhibition of these genes leads to suppression of movement of myeloid cells and decreased activation of granulocytes (Fig. 6A). These analyses further support our hypothesis that inhibition of activation of myeloid cells is the major mechanism for resistance of AEG-1KO mice for developing HCC.

Discussion

The observation that Alb/AEG-1 mice do not develop spontaneous HCC (32) prompted us to hypothesize that AEG-1 is not able to transform hepatocytes, hence it is not required for initial development of HCC. In human HCC cells, overexpression of AEG-1 or knockdown of AEG-1 markedly affects invasion, angiogenesis and metastasis, and in comparison the effects on cell proliferation is significant but small (22). In breast cancer cells modulation of AEG-1 does not affect proliferation at all, rather all phenotypes are reflected in more aggressive behavior, such as invasion and metastasis (23, 24). These findings lead to the

conclusion that the primary role of AEG-1 is to promote aggressive behavior and owing to its profound effect on metastasis, it was named Metadherin (24). Our studies using AEG-1KO mice demonstrate for the first time that even after a mutagenic effect, such as by DEN, AEG-1 is required for initial development of the tumor, at least in the context of HCC. We document that abrogation of NF-κB signaling in hepatocytes and the tumor microenvironment cells, such as macrophages, might be the underlying mechanism that prevents paracrine signaling from macrophages to stimulate mutated hepatocytes to proliferate. Upon DEN treatment a significant decrease in activated NF-κB and STAT3 and IL-6 levels was observed in AEG-1KO livers *versus* WT providing supporting evidence for our hypothesis. In the short-term experiment DEN was able to cause liver damage to both WT and AEG-1KO mice indicating that the tumor-inhibitory effect observed in AEG-1KO mice is not because of ablation of DEN effect. Damaged hepatocytes release factors, such as IL-1α, that activate NF-κB in macrophages leading to secretion of IL-6 that stimulates STAT3 activation in hepatocytes promoting their proliferation (19). In AEG-1KO mice, inhibition of NF-κB activation in macrophages stalls the subsequent processes, therefore, profoundly abrogating initial development of the tumor (Fig. 6B). This scenario might be applicable to other cancers as well since chronic inflammation is a core component of almost all cancers. Indeed, AEG-1KO mice show low basal level of inflammation which might protect them from spontaneous tumorigenesis as observed in aged WT mice.

Multiple studies have documented the important roles of PI3K/AKT, MAPK and Wnt/β-catenin signaling pathways in mediating oncogenic functions of overexpressed AEG-1 (22, 25, 36). However, AEG-1KO hepatocytes do not show abrogated response upon EGF stimulation when compared to WT, and no difference was observed in the activated status of AKT, ERK1/2 and β-catenin in the livers of WT and AEG-1KO mice under basal condition or upon DEN treatment. These observations might be explained by the localization of AEG-1 in normal hepatocytes versus HCC cells. In normal hepatocytes AEG-1 is almost exclusively located in the nucleus (32). In cancer cells overexpressed AEG-1 is monoubiquitinated which facilitates its cytoplasmic accumulation (32, 37). In the cytoplasm overexpressed AEG-1 might exert promiscuous interaction with other signaling molecules leading to their activation, a function that is attributed to oncogenic AEG-1 but not under physiological condition.

The observation that AEG-1 is required for NF-κB activation in macrophages has profound implications in diverse physiological and pathological states. Activation of NF-κB pathways in dendritic cells is essential for their optimal functioning, including antigen processing and presentation (38). Using the human promonocytic cell line U937, it was documented that LPS induces AEG-1 and this induction is required for subsequent NF-κB activation (39). Additionally, NF-κB activation is required for LPS-induced AEG-1 induction thus establishing a positive feedback loop between AEG-1 and NF-κB. NF-κB activation is a key requirement for generating interferon-induced anti-viral immunity. Thus AEG-1 might be a key component regulating immune function. Additionally AEG-1 might be a key regulator of chronic inflammatory diseases.

In summary, our studies unravel a novel and important role of AEG-1 in regulating inflammation and activation of cells in the tumor microenvironment. AEG-1KO mice will

be a valuable tool to interrogate in detail the role of AEG-1 in physiological regulation of immunity and inflammation and diseases generated from deregulation of these systems.

Supplementary Material

Refer to Web version on PubMed Central for supplementary material.

Acknowledgments

DS is the Harrison Endowed Scholar in Cancer Research and Blick scholar. PBF holds the Thelma Newmeyer Corman Chair in Cancer Research.

Financial Support: Present study was supported in part by grants from The James S. McDonnell Foundation (DS) and National Cancer Institute Grants R01 CA138540 (DS) and R01 CA134721 (PBF).

Abbreviations

AEG-1	Astrocyte Elevated Gene-1
DEN	N-nitrosodiethylamine
PB	Phenobarbital
AFP	Alpha-feto protein
HCC	Hepatocellular carcinoma
LPS	Lipopolysaccharide

References

1. El-Serag HB. Hepatocellular carcinoma. N Engl J Med. 2011; 365:1118–27. [PubMed: 21992124]
2. Berasain C, Castillo J, Perugorria MJ, Latasa MU, Prieto J, Avila MA. Inflammation and liver cancer: new molecular links. Ann N Y Acad Sci. 2009; 1155:206–21. [PubMed: 19250206]
3. Pikarsky E, Porat RM, Stein I, Abramovitch R, Amit S, Kasem S, et al. NF-kappaB functions as a tumour promoter in inflammation-associated cancer. Nature. 2004; 431:461–6. [PubMed: 15329734]
4. Karin M, Ben-Neriah Y. Phosphorylation meets ubiquitination: the control of NF-[kappa]B activity. Annu Rev Immunol. 2000; 18:621–63. [PubMed: 10837071]
5. Liu P, Kimmoun E, Legrand A, Sauvanet A, Degott C, Lardeux B, et al. Activation of NF-kappa B, AP-1 and STAT transcription factors is a frequent and early event in human hepatocellular carcinomas. J Hepatol. 2002; 37:63–71. [PubMed: 12076863]
6. Tai DI, Tsai SL, Chang YH, Huang SN, Chen TC, Chang KS, et al. Constitutive activation of nuclear factor kappaB in hepatocellular carcinoma. Cancer. 2000; 89:2274–81. [PubMed: 11147598]
7. Tai DI, Tsai SL, Chen YM, Chuang YL, Peng CY, Sheen IS, et al. Activation of nuclear factor kappaB in hepatitis C virus infection: implications for pathogenesis and hepatocarcinogenesis. Hepatology. 2000; 31:656–64. [PubMed: 10706556]
8. Hosel M, Quasdorff M, Wiegmann K, Webb D, Zedler U, Broxtermann M, et al. Not interferon, but interleukin-6 controls early gene expression in hepatitis B virus infection. Hepatology. 2009; 50:1773–82. [PubMed: 19937696]
9. Mandrekar P, Szabo G. Signalling pathways in alcohol-induced liver inflammation. J Hepatol. 2009; 50:1258–66. [PubMed: 19398236]
10. Kim HR, Lee SH, Jung G. The hepatitis B viral X protein activates NF-kappaB signaling pathway through the up-regulation of TBK1. FEBS letters. 2010; 584:525–30. [PubMed: 19958770]

11. Lu B, Guo H, Zhao J, Wang C, Wu G, Pang M, et al. Increased expression of iASPP, regulated by hepatitis B virus X protein-mediated NF-kappaB activation, in hepatocellular carcinoma. Gastroenterology. 2010; 139:2183–94. e5. [PubMed: 20600029]
12. Schwabe RF, Seki E, Brenner DA. Toll-like receptor signaling in the liver. Gastroenterology. 2006; 130:1886–900. [PubMed: 16697751]
13. Shi H, Kokoeva MV, Inouye K, Tzameli I, Yin H, Flier JS. TLR4 links innate immunity and fatty acid-induced insulin resistance. J Clin Invest. 2006; 116:3015–25. [PubMed: 17053832]
14. Haybaeck J, Zeller N, Wolf MJ, Weber A, Wagner U, Kurrer MO, et al. A lymphotoxin-driven pathway to hepatocellular carcinoma. Cancer Cell. 2009; 16:295–308. [PubMed: 19800575]
15. Maeda S, Kamata H, Luo JL, Leffert H, Karin M. IKKbeta couples hepatocyte death to cytokine-driven compensatory proliferation that promotes chemical hepatocarcinogenesis. Cell. 2005; 121:977–90. [PubMed: 15989949]
16. Luedde T, Beraza N, Kotsikoris V, van Loo G, Nenci A, De Vos R, et al. Deletion of NEMO/IKKgamma in liver parenchymal cells causes steatohepatitis and hepatocellular carcinoma. Cancer Cell. 2007; 11:119–32. [PubMed: 17292824]
17. He G, Yu GY, Temkin V, Ogata H, Kuntzen C, Sakurai T, et al. Hepatocyte IKKbeta/NF-kappaB inhibits tumor promotion and progression by preventing oxidative stress-driven STAT3 activation. Cancer cell. 2010; 17:286–97. [PubMed: 20227042]
18. Park EJ, Lee JH, Yu GY, He G, Ali SR, Holzer RG, et al. Dietary and genetic obesity promote liver inflammation and tumorigenesis by enhancing IL-6 and TNF expression. Cell. 2010; 140:197–208. [PubMed: 20141834]
19. Sakurai T, He G, Matsuzawa A, Yu GY, Maeda S, Hardiman G, et al. Hepatocyte necrosis induced by oxidative stress and IL-1 alpha release mediate carcinogen-induced compensatory proliferation and liver tumorigenesis. Cancer Cell. 2008; 14:156–65. [PubMed: 18691550]
20. Naugler WE, Sakurai T, Kim S, Maeda S, Kim K, Elsharkawy AM, et al. Gender disparity in liver cancer due to sex differences in MyD88-dependent IL-6 production. Science. 2007; 317:121–4. [PubMed: 17615358]
21. Sarkar D, Fisher PB. AEG-1/MTDH/LYRIC: Clinical Significance. Adv Cancer Res. 2013; 120:39–74. [PubMed: 23889987]
22. Yoo BK, Emdad L, Su ZZ, Villanueva A, Chiang DY, Mukhopadhyay ND, et al. Astrocyte elevated gene-1 regulates hepatocellular carcinoma development and progression. J Clin Invest. 2009; 119:465–77. [PubMed: 19221438]
23. Hu G, Chong RA, Yang Q, Wei Y, Blanco MA, Li F, et al. MTDH activation by 8q22 genomic gain promotes chemoresistance and metastasis of poor-prognosis breast cancer. Cancer Cell. 2009; 15:9–20. [PubMed: 19111877]
24. Brown DM, Ruoslahti E. Metadherin, a cell surface protein in breast tumors that mediates lung metastasis. Cancer Cell. 2004; 5:365–74. [PubMed: 15093543]
25. Emdad L, Lee SG, Su ZZ, Jeon HY, Boukerche H, Sarkar D, et al. Astrocyte elevated gene-1 (AEG-1) functions as an oncogene and regulates angiogenesis. Proc Natl Acad Sci U S A. 2009; 106:21300–5. [PubMed: 19940250]
26. Lee SG, Su ZZ, Emdad L, Sarkar D, Fisher PB. Astrocyte elevated gene-1 (AEG-1) is a target gene of oncogenic Ha-ras requiring phosphatidylinositol 3-kinase and c-Myc. Proc Natl Acad Sci U S A. 2006; 103:17390–5. [PubMed: 17088530]
27. Villanueva A, Newell P, Chiang DY, Friedman SL, Llovet JM. Genomics and signaling pathways in hepatocellular carcinoma. Semin Liver Dis. 2007; 27:55–76. [PubMed: 17295177]
28. He XX, Chang Y, Meng FY, Wang MY, Xie QH, Tang F, et al. MicroRNA-375 targets AEG-1 in hepatocellular carcinoma and suppresses liver cancer cell growth in vitro and in vivo. Oncogene. 2012; 31:3357–69. [PubMed: 22056881]
29. Zhu K, Dai Z, Pan Q, Wang Z, Yang GH, Yu L, et al. Metadherin Promotes Hepatocellular Carcinoma Metastasis through Induction of Epithelial-Mesenchymal Transition. Clin Cancer Res. 2011; 17:7294–302. [PubMed: 21976539]
30. Gong Z, Liu W, You N, Wang T, Wang X, Lu P, et al. Prognostic significance of metadherin overexpression in hepatitis B virus-related hepatocellular carcinoma. Oncol Rep. 2012; 27:2073–9. [PubMed: 22470125]

31. Yoo BK, Gredler R, Vozhilla N, Su ZZ, Chen D, Forcier T, et al. Identification of genes conferring resistance to 5-fluorouracil. Proc Natl Acad Sci U S A. 2009; 106:12938–43. [PubMed: 19622726]
32. Srivastava J, Siddiq A, Emdad L, Santhekadur P, Chen D, Gredler R, et al. Astrocyte elevated gene-1 (AEG-1) promotes hepatocarcinogenesis: novel insights from a mouse model. Hepatology. 2012; 56:1782–91. [PubMed: 22689379]
33. Emdad L, Sarkar D, Su ZZ, Randolph A, Boukerche H, Valerie K, et al. Activation of the nuclear factor kappaB pathway by astrocyte elevated gene-1: implications for tumor progression and metastasis. Cancer Res. 2006; 66:1509–16. [PubMed: 16452207]
34. Sarkar D, Park ES, Emdad L, Lee SG, Su ZZ, Fisher PB. Molecular basis of nuclear factor-kappaB activation by astrocyte elevated gene-1. Cancer Res. 2008; 68:1478–84. [PubMed: 18316612]
35. Alexia C, Poalas K, Carvalho G, Zemirli N, Dwyer J, Dubois SM, et al. The endoplasmic reticulum acts as a platform for ubiquitylated components of nuclear factor kappaB signaling. Sci Signal. 2013; 6:ra79. [PubMed: 24003256]
36. Lee SG, Su ZZ, Emdad L, Sarkar D, Franke TF, Fisher PB. Astrocyte elevated gene-1 activates cell survival pathways through PI3K-Akt signaling. Oncogene. 2008; 27:1114–21. [PubMed: 17704808]
37. Thirkettle HJ, Girling J, Warren AY, Mills IG, Sahadevan K, Leung H, et al. LYRIC/AEG-1 is targeted to different subcellular compartments by ubiquitinylation and intrinsic nuclear localization signals. Clin Cancer Res. 2009; 15:3003–13. [PubMed: 19383828]
38. Andreakos E, Williams RO, Wales J, Foxwell BM, Feldmann M. Activation of NF-kappaB by the intracellular expression of NF-kappaB-inducing kinase acts as a powerful vaccine adjuvant. Proc Natl Acad Sci U S A. 2006; 103:14459–64. [PubMed: 16971487]
39. Khuda II, Koide N, Noman AS, Dagvadorj J, Tumurkhuu G, Naiki Y, et al. Astrocyte elevated gene-1 (AEG-1) is induced by lipopolysaccharide as toll-like receptor 4 (TLR4) ligand and regulates TLR4 signalling. Immunology. 2009; 128:e700–6. [PubMed: 19740331]

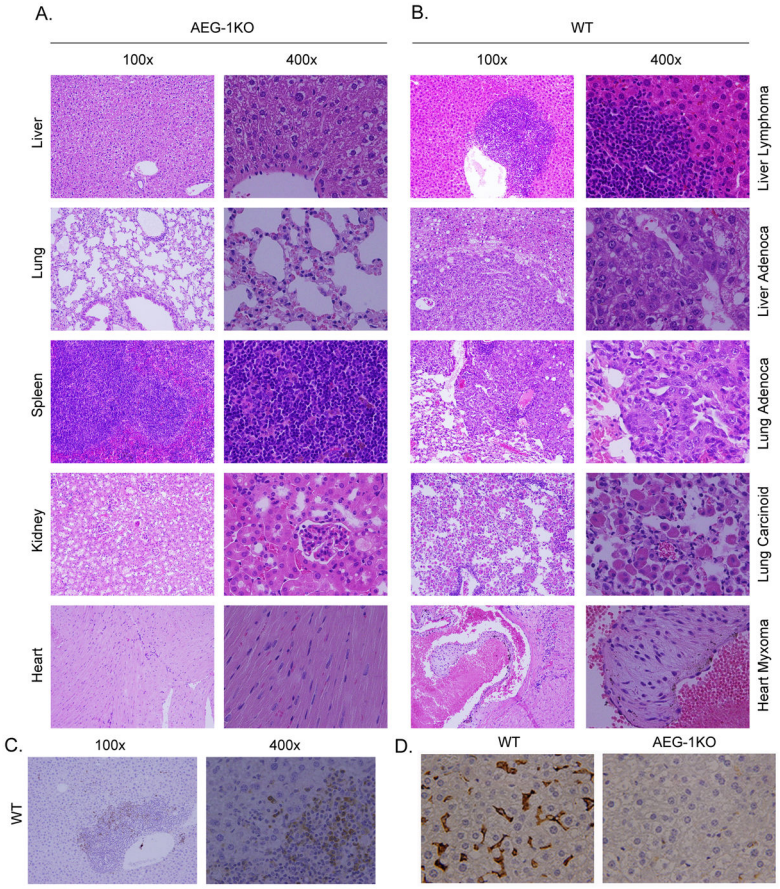

Fig. 1.

AEG-1KO mice are resistant to age-associated spontaneous tumorigenesis. A. H & E staining of the indicated tissue sections of aged (16 m) AEG-1KO mouse demonstrating maintenance of normal histology and architecture. B. H & E staining of sections of liver, lung and heart of aged (16 m) WT mouse showing tumors. C. Immunohistochemical staining for AEG-1 in liver lymphoma of WT mouse. D. F4/80 staining for macrophages in liver sections of aged (16 m) WT and AEG-1KO mouse.

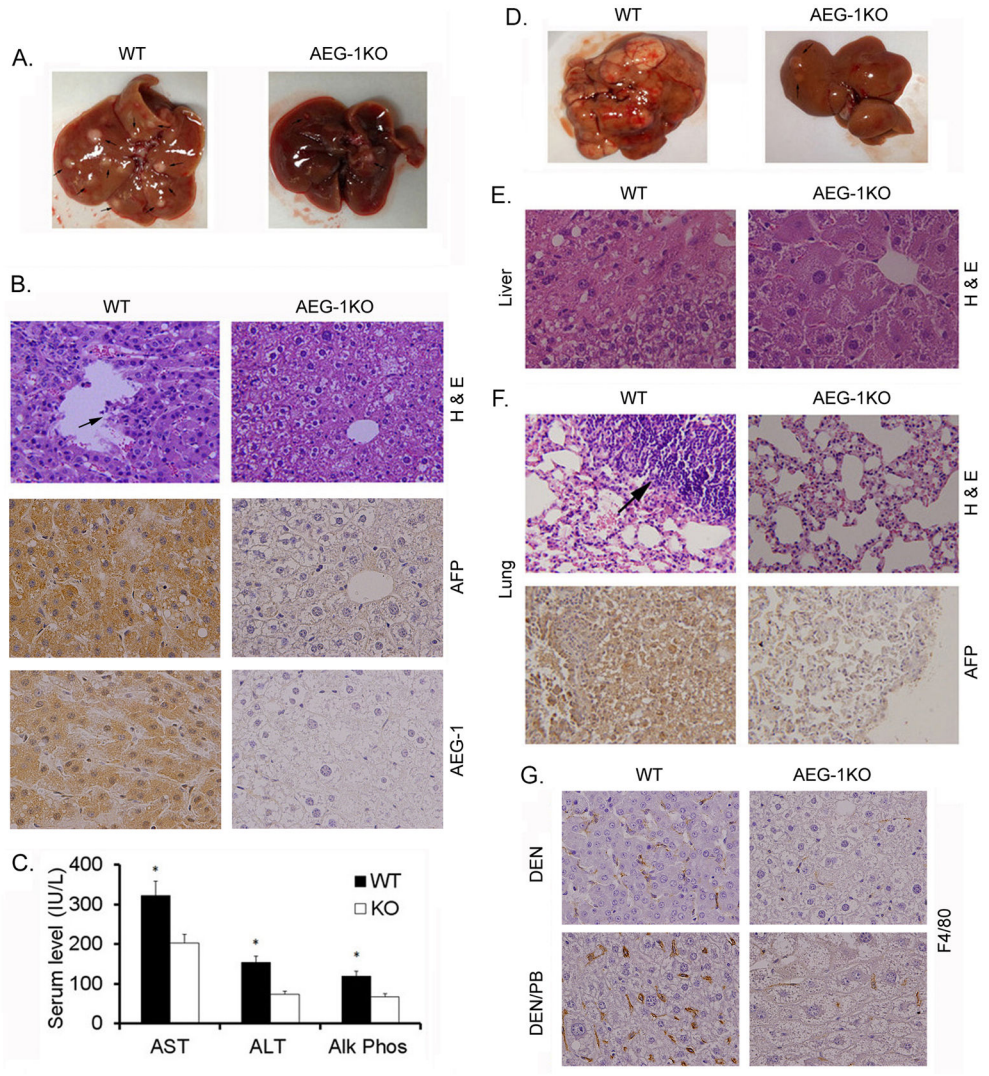

Fig. 2.

AEG-1KO mouse is resistant to experimental hepatocarcinogenesis. A. Representative photograph of the livers of WT and AEG-1KO mice 32 weeks after DEN injection. B, top panel, H & E staining of liver sections; middle panel, AFP staining of the liver sections; bottom panel, AEG-1 staining of the liver sections. These samples were collected at 32 weeks after DEN injection. C. Serum levels of the indicated liver enzymes at the end of the study. AST: aspartate aminotransferase, ALT; alanine aminotransferase and Alk Phos: alkaline phosphatase. Data represent mean ± SEM. n = 12 for WT and n = 8 for AEG-1KO. *: $p<0.01$. D. Representative photograph of the livers of WT and AEG-1KO mice 28 weeks after initial DEN injection receiving PB in drinking water. E. H & E staining of liver sections at 28 weeks. F. top panel, H & E staining of the lungs showing lung metastasis in WT mouse; bottom panel, AFP staining of a metastatic lung tumor in WT mouse. G. F4/80 staining for macrophages in liver sections of WT and AEG-1KO mice treated with DEN alone (top panels) or DEN/PB (bottom panels).

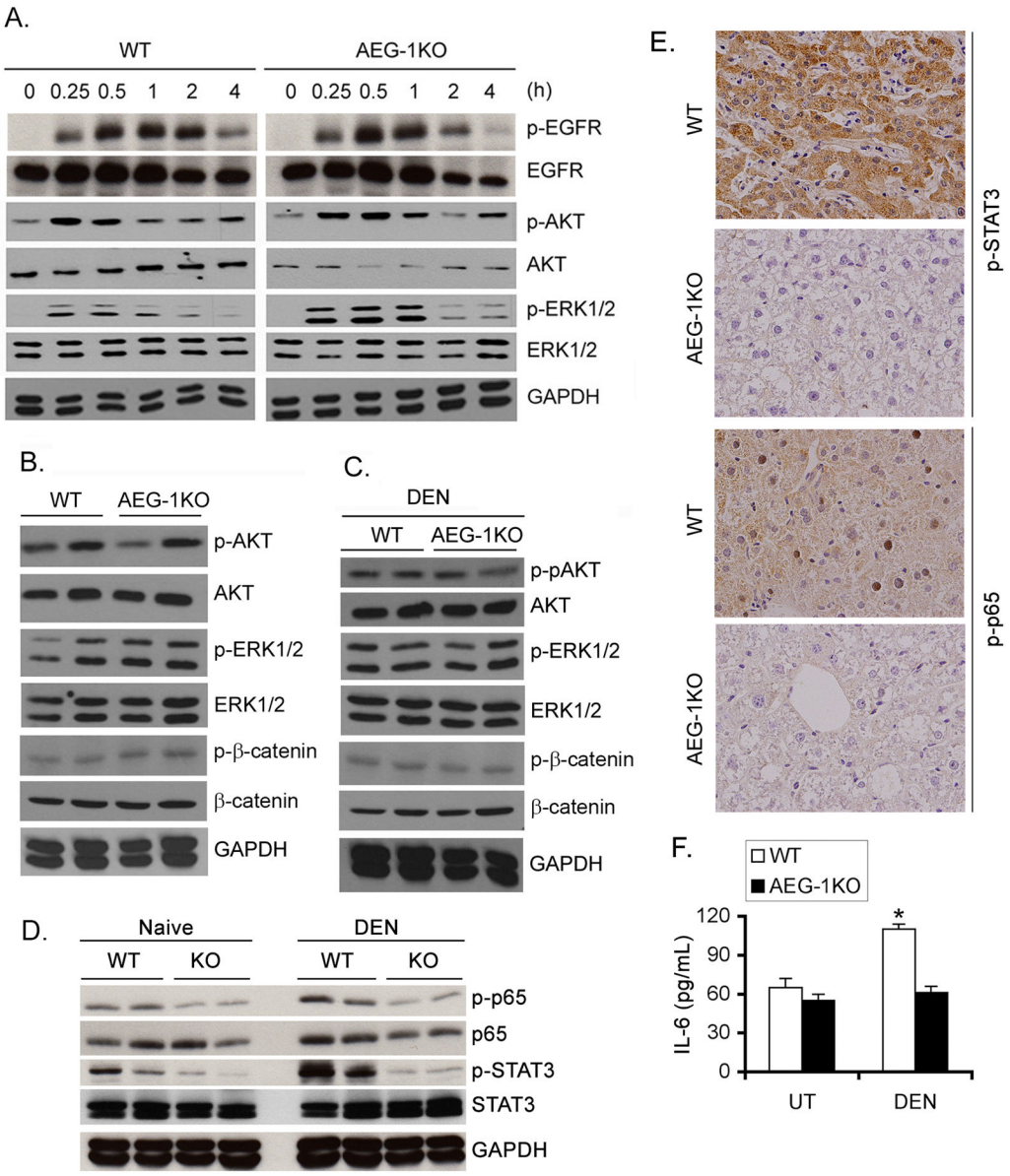

Fig. 3.

NF-κB and STAT3 activation is inhibited in AEG-1KO mouse. A. WT and AEG-1KO hepatocytes were treated with EGF (50 ng/mL) for the indicated time points and Western blotting was performed for the indicated proteins. B. Western blot was performed for the indicated proteins using liver lysates from adult WT and AEG-1KO mice. C. Western blotting was performed for the indicated proteins using liver lysates from DEN-treated WT and AEG-1KO mice at the end of the study. D. Western blotting was performed for the indicated proteins using liver lysates from naïve and DEN-treated WT and AEG-1KO mice at the end of the study. For B–D, each lane represents one independent mouse. E. DEN-treated liver sections were stained for p-STAT3 and p-p65 NF-κB at the end of the study. F. IL-6 protein level was measured in DEN-treated liver homogenates by ELISA. Data represent mean ± SEM. n = 5. *: $p<0.01$.

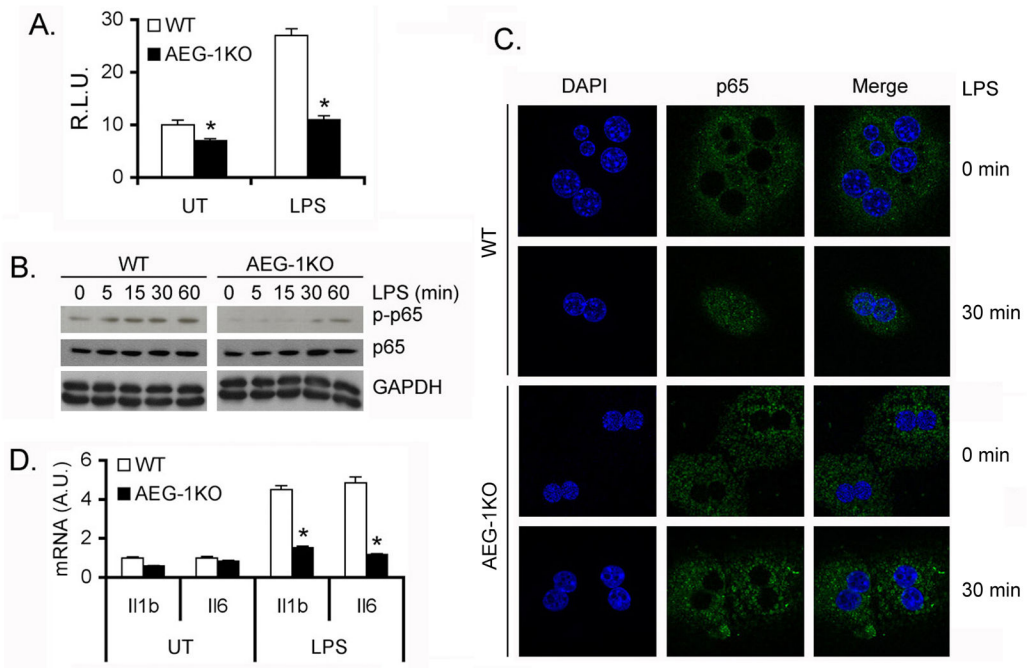

Fig. 4.

NF-κB activation is inhibited in AEG-1KO hepatocytes. A. NF-κB luciferase reporter activity was measured in WT and AEG-1KO hepatocytes. Firefly luciferase activity was normalized by Renilla luciferase activity. The activity of empty pGL3-basic vector was considered as 1. R.L.U.: Relative luciferase units. Data represent mean ± SEM of three independent experiments. *: $p<0.01$. B. WT and AEG-1KO hepatocytes were treated with LPS for the indicated time points and Western blotting was performed for the indicated proteins. C. Immunofluorescence followed by confocal microscopy of WT and AEG-1KO hepatocytes after LPS treatment for 30 min showing p65 nuclear translocation. D. WT and AEG-1KO hepatocytes were treated with LPS for 4 h and the mRNA level of Il1b and Il6 was measured by Taqman Q-RT-PCR. Data represent mean ± SEM of three independent experiments. *: $p<0.01$.

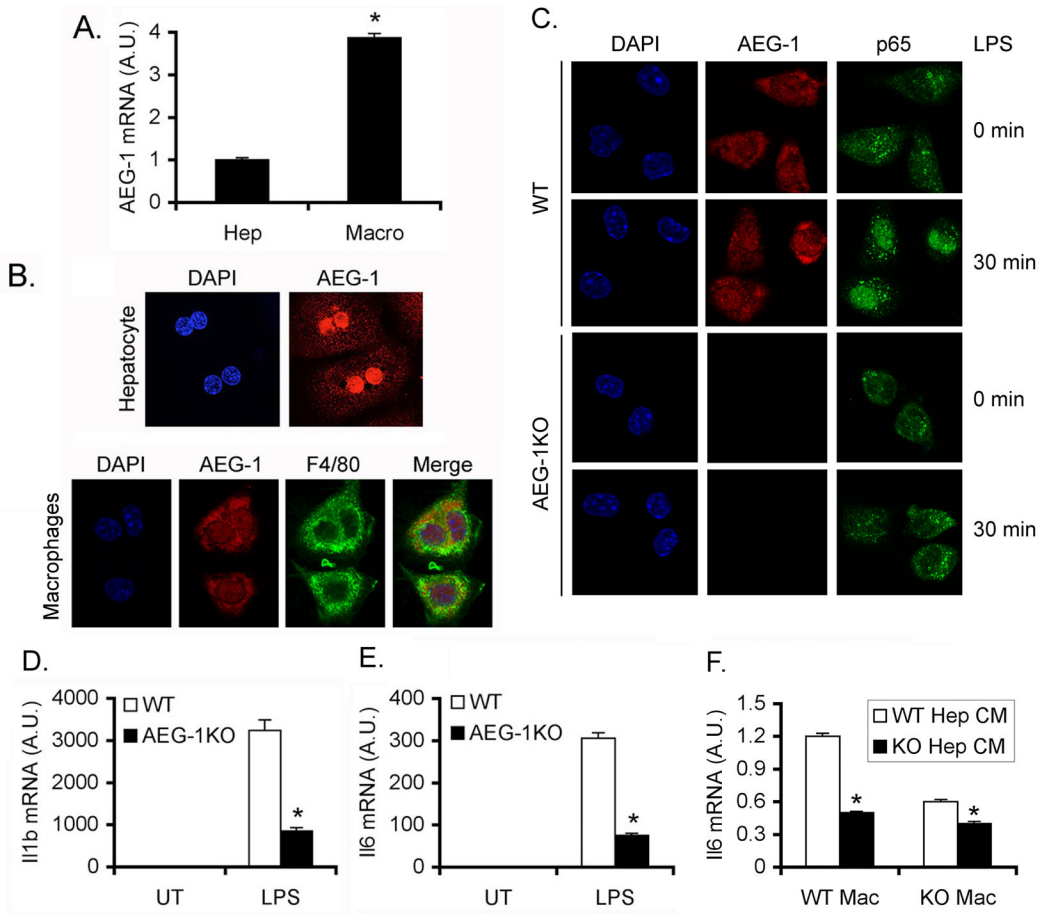

Fig. 5.

NF-κB activation is inhibited in AEG-1KO macrophages. A. AEG-1 mRNA level in hepatocytes and macrophages of WT mice measured by Taqman Q-RT-PCR. A.U.: arbitrary unit. Data represent mean ± SEM of three independent experiments. *: $p<0.01$. B. Immunofluorescence staining showing subcellular localization of AEG-1 in WT hepatocytes and macrophages. F4/80 staining was performed in macrophages to demonstrate authenticity of purification. C. Immunofluorescence followed by confocal microscopy of WT and AEG-1KO macrophages after LPS treatment for 30 min showing p65 nuclear translocation. D–E. WT and AEG-1KO macrophages were treated with LPS for 12 h and the mRNA levels of Il1b (D) and Il6 (E) were measured by Taqman Q-RT-PCR. F. WT and AEG-1KO macrophages were treated with conditioned media (CM) from LPS-treated WT and AEG-1KO hepatocytes and Il6 mRNA expression was measured by Taqman Q-RT-PCR 4 h later. For D–F, data represent mean ± SEM of three independent experiments. *: $p<0.01$.

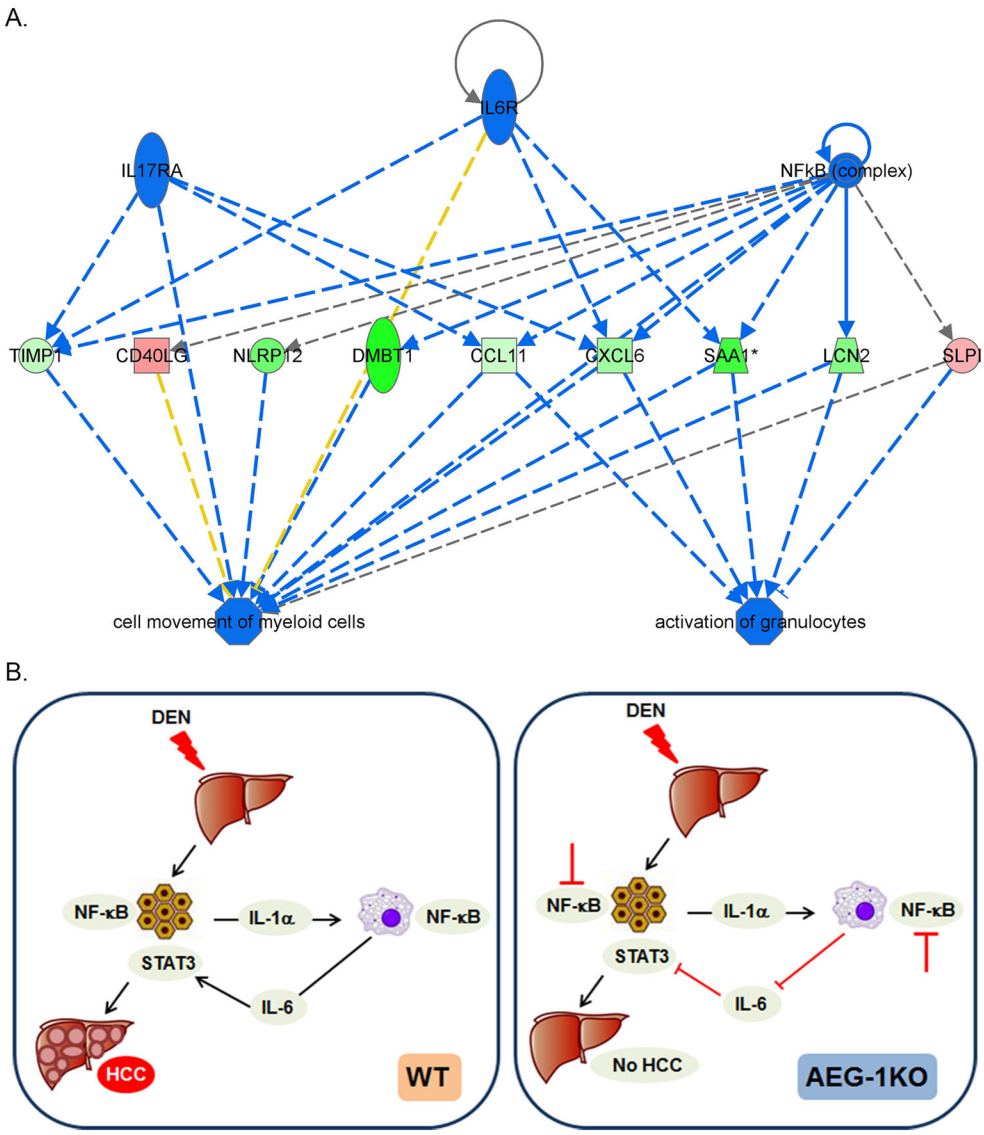

Fig. 6.

Molecular mechanism rendering AEG-1KO mice resistant to HCC. A. Functional endpoints, analyzed by Ingenuity pathway analysis, that are inhibited in AEG-1KO mice. Blue line: inhibition; red line: activation; yellow line: finding inconsistent with state of downstream molecules; gray line: effect not predicted. Green color: downregulation of expression; red color: upregulation of expression. B. Schematic representation of the molecular mechanism of resistance of AEG-1KO mice to HCC. In WT mice DEN-induced hepatocyte injury leads to IL-1α production that activates NF-κB in the macrophages leading to production of IL-6. IL-6 activates STAT3 in hepatocytes facilitating proliferation of the mutated cells leading to HCC. In AEG-1KO mice NF-κB activation is inhibited in hepatocytes and macrophages thereby inhibiting IL-6 production and STAT3 activation. As a consequence, HCC development is significantly abrogated.

Cancer Res. Author manuscript; available in PMC 2015 November 01.

Table 1

Number of liver nodules and lung metastasis in DEN- and PB-treated WT and AEG-1KO mice.

	ID#	Total no. of nodules	Lung Mets		ID#	Total no. of nodules	Lung Mets
WT	1	Entire liver	Yes	**AEG-1KO**	1	0	No
	2	5	No		2	0	No
	3	34	No		3	0	No
	4	42	No		4	0	No
	5	Entire liver	Yes		5	3	No
	6	18	No		6	10	No
	7	Entire liver	Yes		7	3	No
	8	Entire liver	Yes		8	3	No
	9	5	No		9	0	No
	10	53	Yes		10	0	No
	11	17	Yes		11	0	No
	12	15	No		12	11	No
	13	0	No		13	0	No
	14	11	No		14	0	No
	15	26	No		15	0	No
	16	37	Yes		16	0	No
	17	3	No		17	0	No
	18	Entire liver	Yes		18	0	No
	19	Entire liver	Yes		19	0	No
	20	19	No		20	0	No
	21	24	Yes		21	0	No
	22	48	Yes		22	3	No
	23	16	Yes		23	0	No